Spectral Analysis of Epicardial 60-lead Electrograms in Dogs during Acute Myocardial Ischemia

Yukio HOSOYA, M.D., Ph.D.*, Kozue IKEDA, M.D., Ph.D.**,
Michiyasu YAMAKI, M.D., Ph.D.**, and Isao KUBOTA, M.D., Ph.D.**

Abstract : Effects of acute myocardial ischemia on each frequency component over an entire cardiac cycle were analyzed. Sixty-lead epicardial electrograms were recorded before and after coronary occlusion in 7 dogs. Signal averaging and fast Fourier transform were performed on the electrograms, and then inverse transform was done for five frequency ranges. During the entire cardiac cycle, integrations of absolute value of reconstructed waveform were calculated and displayed as filtered QRST area maps. In addition, root-mean-square electrograms were calculated from leads in the ischemic region. Myocardial ischemia significantly diminished the low-frequency (0-25Hz) components only in the initial QRS, while markedly increased these components in the last half of QRS complex and ST segment. In contrast, myocardial ischemia significantly decreased both mid- and high-frequency (25-250Hz) components in the early to middle portion of QRS complex, whereas markedly increased high-frequency (80-250Hz) potentials in the terminal QRS.
Key words : myocardial ischemia, epicardial electrogram, signal-averaged electrogram, spectral analysis

Introduction

Effects of myocardial ischemia on high frequency potentials within QRS complex are still controversial. Time-domain analysis and spectral analysis revealed reduction of high-frequency energy within QRS complex during acute myocardial ischemia[1-4] or in patients with previous MI[5-7]. In our previous studies[8, 9], we also demonstrated that high frequency potentials within QRS complex were reduced in patients with previous MI, or in dogs with 4-week-old MI. On the other hand, several researchers reported that high frequency components within QRS complex were increased during acute myocardial ischemia[10], or in patients with previous MI[11]. Many researchers[12-15] have reported that high frequency potentials were increased in terminal QRS complex and/or early ST segment in patients with previous MI, especially in patients with ventricular tachycardia.

In the previous studies[1, 3, 4], epicardial electrogram in the ischemic region was recorded by a single bipolar electrode, and epicardial distributions of low- or high-frequency component are unclear. In addition, effects of myocardial ischemia on the temporal distribution of epicardial high-frequency electrogram are not fully investigated so far. There are few studies about the spectral analysis of multiple-lead epicardial electrograms in the condition of acute myocardial ischemia. For the further assessment of the effects of ischemia on both high- and low-frequency potentials, we obtained 60-lead epicardial electrograms directly from the ischemic region and non-ischemic region. Then, we performed the spectral analysis of 60-lead epicardial electrograms obtained during acute myocardial ischemia. By this technique, we can get

* Department of Nursing, Faculty of Health Science, Yamagata Prefectural University of Health Science. 260 Kamiyanagi, Yamagata, Yamagata 990-2212, Japan
** The First Department of Internal Medicine, Yamagata University School of Medicine.

information about epicardial spatial distribution of each frequency potential over the entire cardiac cycle. In addition, we investigated the effect of myocardial ischemia on the temporal distributions of both high- and low-frequency potentials.

Methods

Experimental protocol

Seven adult mongrel dogs (weight, 14 to 18kg) were anesthetized with an intravenous administration of sodium pentobarbital (30mg/kg body wt.), and artificially ventilated through a cuffed endotracheal tube with a constant-volume ventilator. Small additional doses of pentobarbital were administered as required during the experiment. The heart was exposed by a midsternal thoracotomy and suspended in a pericardial cradle. Sinus node was crushed, and a bipolar stimulating electrode was attached to the right atrium. The heart was paced at a cycle length of 428 msec (140beats/min) with 2 msec duration square-wave stimuli at twice diastolic threshold intensity. A proximal part of the left anterior descending coronary artery (LAD) at the level just distal of its first diagonal branch was dissected free of epicardium, and a mechanical occluder was placed around the vessel.

Sixty silver wire unipolar electrodes attached to a nylon stocking were stretched over the heart for recording cardiac surface electrograms. The electrode array had six rows (1 to 6) and ten columns (A through J) as previously reported in detail elsewhere[9, 16]. Each cardiac surface electrode was referenced to Wilson's central terminal. All 60-lead electrograms were recorded simultaneously with a sampling interval of 1 msec using a data recording system (CD-0055, Chunichi denshi Corp., Nagoya, Japan)[9, 16-18]. Epicardial mapping data were sampled for 8 seconds and transmitted to a personal computer (NEC PC-9801VX4, Nippon Electric Corp., Tokyo, Japan) [9, 13]. Sixty-lead epicardial electrograms were recorded every 3 minutes for 10 times before coronary occlusion (control phase), and 1, 3, 5, 7, 10, 15, 30, 45, and 60 minutes after coronary occlusion (ischemic phase). All experiments were performed in the laboratory of Yamagata University School of Medicine.

Analysis of 60-lead epicardial electrograms

Epicardial electrograms were averaged to reduce a random noise with the personal computer as previously reported in detail[8, 9, 13, 19]. The averaging was achieved with the use of a cross-correlation function in a time domain to reject ectopic beats and grossly noisy signals. The number of beats averaged was 18. Root-mean-square (RMS) values of 60-lead electrograms were determined as follows :

$$r(t) = \sqrt{\frac{1}{N}\sum_{e=1}^{N} f(t,e)^2}\ , \quad \textit{Equation } 1$$

where N means the number of leads, t is a sample point, e is a lead, $f\ (t,\ e)$ indicates the amplitude of epicardial electrogram at sample point t of an e lead, and $r\ (t)$ is 60-lead RMS value at sample point t. RMS voltage of 60-lead averaged electrograms versus time curve was plotted to determine visually an onset and offset of QRS complex and an end of T wave. The amplitude of ST segment was measured at 40msec after the offset of the QRS complex, and 2.0mV or greater additional ST elevation induced by myocardial ischemia was considered to be significant.

Baseline correction was performed on the electrograms of an entire cardiac cycle by triangulation to ensure that the first and last data points were isopotential. For analysis with a fast Fourier transform (FFT), data interval was padded with zeros for a total of 1,024points. A time series f (t) representing the averaged electrogram of the entire cardiac cycle was subjected to a 1,024-point FFT analysis to produce a frequency series $F(\omega)$. A product of $F(\omega)$ with a frequency response function $H(\omega)$ was computed to produce a filtered waveform $G(\omega)$ in a frequency domain.

$G(\omega)=F(\omega)\cdot H(\omega)$, where $H(\omega)$ is given by the following function, previously reported by Abboud et al.[1-4, 20]

$$H(\omega) = \left(1/\sqrt{1+(W_L/\omega)^n}\right)\left\{1-\left(1/\sqrt{1+(W_H/\omega)^m}\right)\right\},$$

Equation 2

with W_L and W_H being a low and high cut-off frequency of the filter. We used 5 frequency ranges ;

(1) 0-25, (2) 25-40, (3) 40-80, (4) 80-150, and (5) 150-250 Hz. Parameters (m-n) were (1) 1-10, (2) 10-16, (3) 16-32, (4) 32-60, and (5) 60-100, respectively. A filtered electrogram g(t) was produced by transformation (inverse FFT) of the signal $G(\omega)$ from the frequency domain back to the time domain.

From the beginning to the end of entire cardiac cycle, time integration of absolute value of reconstructed waveform was calculated for each of the 5 frequency ranges. Epicardial distributions of these areas were expressed as filtered QRST area (fQRST) maps (0-25, 25-40, 40-80, 80-150, and 150-250Hz, respectively).

Individual and group mean fAQRST maps were plotted. Individual maps were constructed from each subject's fAQRST values at each lead site. On the other hand, group mean maps were constructed from the arithmetic average of the respective fAQRST values from all dogs at each electrode site. To delineate the changes in spatial distributions, difference maps were constructed by subtracting the mean fAQRST map before coronary occlusion from that after coronary occlusion. In difference maps, solid lines represent the area where fAQRST values were increased after coronary occlusion, while dotted lines represent the area where fAQRST values were decreased after coronary occlusion compared to those before occlusion.

Statistical analysis

Quantitative data were expressed as mean ± SEM. Statistical analysis was performed with the use of a computer-based statistical software package (SAS : Statistical Analysis System, SAS Institute Inc., Cary, N.C., U.S.A.). Analysis of variance (ANOVA) was employed with SAS general linear model's (GLM) procedure. A value of $p<0.05$ was considered statistically significant.

Results

Figure 1 shows 60-lead epicardial electrograms in a representative case. Upper panel(A) represents electrograms just before coronary occlusion, and lower panel(B) shows electrograms of 10 minutes after coronary occlusion. Epicardial leads with significant ST segment elevation were surrounded by a dashed line. By myocardial ischemia, significant ST elevation was induced in leads of left ventricular (LV) anterior wall and apex, corresponding to the territory of the LAD (A1-6, B1-6, C1-6, D1-6, and E3-6 leads). In this study, the electrodes with significant ST elevation were defined as ischemic region, and the other leads without the significant ST elevation were defined as non-ischemic region.

Significant ST segment elevation was consistently observed over the LAD-perfused region after coronary occlusion in all 7 dogs. Figure 2 summarized the sites of epicardial electrodes with significant ST segment elevation in all cases. Numerals represent the number of dogs which

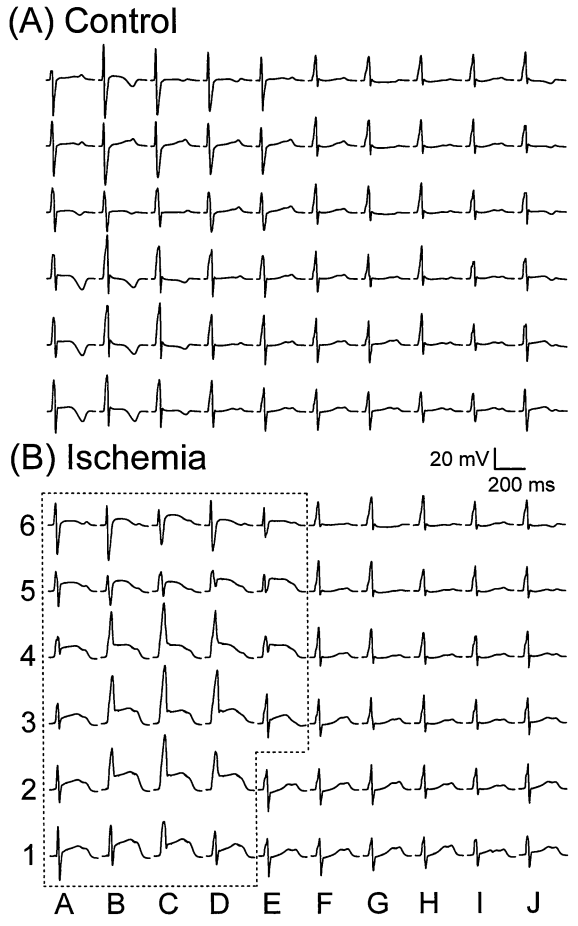

Figure 1 60-lead unipolar epicardial electrograms in a representative dog.

Panel A shows electrograms of just before coronary occlusion, and panel B represents electrograms recorded at 10 minutes after coronary occlusion. Epicardial leads with significant ST segment elevation were surrounded by dashed lines. Myocardial ischemia induced significant ST elevation in leads of left ventricular anterior wall and apex.

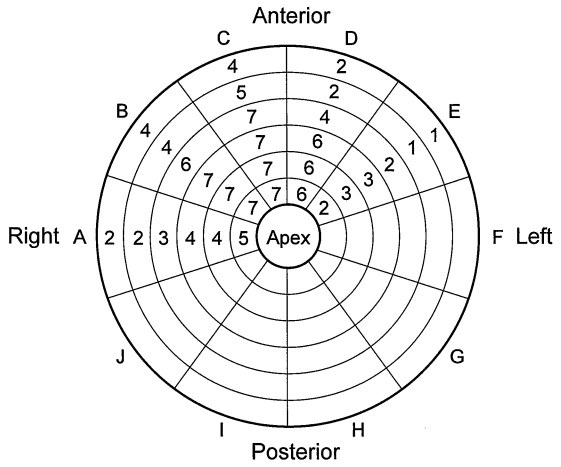

Figure 2 Sites of epicardial leads with significant ST elevation in all 7 dogs.

An apical polar projection of ventricles is shown, with left ventricular apex in center. Numerals represent the number of dogs which showed significant ST segment elevation at the lead point after coronary occlusion.

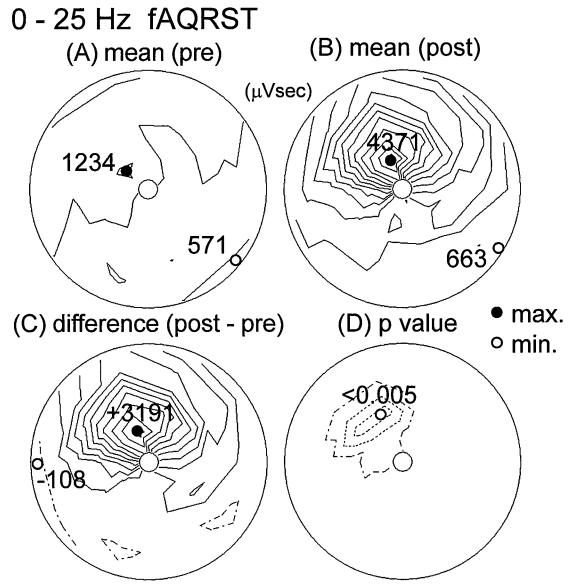

Figure 3 Effect of myocardial ischemia on 0-25 Hz fAQRST map.

Changes in low frequency potentials by LAD occlusion: mean maps of just before (panel A) and 10 minutes after coronary occlusion (panel B), difference map (post - pre) (panel C), and p value map (pre vs. post) (panel D). Closed circle indicates a site of maximum and open circle indicates a site of minimum. The maximum and minimum values are indicated on each map. In the p value map, the leads where p values were less than 0.05 are surrounded by a dashed line, and 2 dotted lines indicate the leads where p values were less than 0.01, 0.005, respectively.

fAQRST : filtered QRST area.

showed significant ST elevation at the lead point. ST elevation was observed in LV anterior wall and apex (especially, the leads of A1-3, B1-B6, C1-C6, D1-D4).

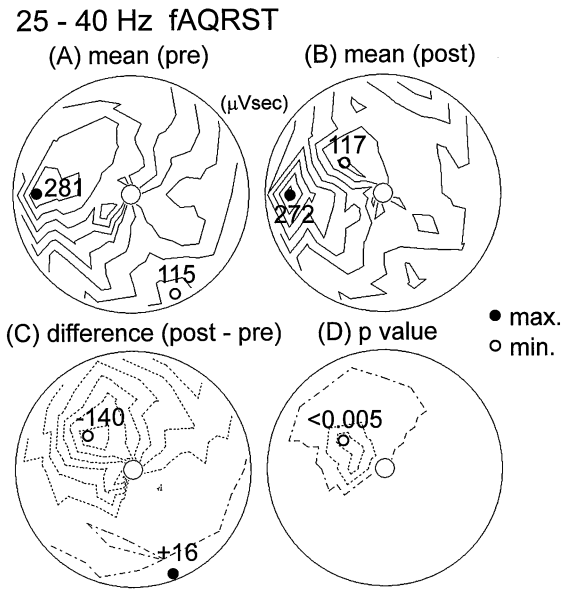

Figure 4 Effect of ischemia on 25-40 Hz fAQRST map.

The figure shows mean maps of just before (panel A) and 10 minutes after coronary occlusion (panel B), difference map (post-pre) (panel C), and p value map (pre vs. post) (panel D).

Epicardial distribution of fAQRST values in each frequency range

Figure 3 illustrates the comparison of 0-25Hz fAQRST map : mean maps of just before (panel A) and 10 minutes after coronary occlusion (panel B), difference map (post-pre) (panel C), and p value map (pre vs. post) (panel D). Values of fAQRST represent the overall amplitude of each frequency component in the entire cardiac cycle at each electrode. Mean values of 0-25Hz fAQRST were compared statistically at each lead point by the use of ANOVA with Scheffe's test. In p value map, the leads with p values less than 0.05 were surrounded by a dashed line. Two dotted lines indicate the leads where p values were less than 0.01 or 0.005, respectively. As shown in the difference map and p value map (panel C and D), low frequency (0-25Hz) fAQRST values were increased significantly in the ischemic region after LAD occlusion. In contrast, in the non-ischemic region, there were no significant differences in 0-25Hz fAQRST values after coronary occlusion.

Figure 4 represents the comparison of 25-40 Hz fAQRST map : mean maps of just before (panel A) and 10 minutes after coronary occlusion (panel B), difference map (post-pre) (panel C), and p value map (pre vs. post) (panel D). As shown in the difference

map and p value map (panel C and D), 25-40Hz fAQRST values were decreased significantly in the ischemic region after coronary occlusion. However, in the non-ischemic region, no significant differences were observed in 25-40Hz fAQRST values after LAD occlusion.

Figure 5 summarized the effects of acute ischemia on 40-80, 80-150, and 150-250Hz fAQRST map. Because the patterns of these mean maps were similar to those of 25-40Hz fAQRST map, only the difference and p value maps were displayed in this figure. In the LAD perfused region, acute myocardial ischemia caused significant decreases in 40-80, 80-150, and 150-250Hz fAQRST values. Alternatively, in the non-ischemic region, no significant differences were seen in 40-80, 80-150, and 150-250Hz fAQRST values after coronary occlusion.

Temporal distributions of each frequency component

RMS voltage of the epicardial electrogram versus time curve was plotted according to equation 1 based on the epicardial electrodes placed in the ischemic region (RMSi electrogram) or non-ischemic region (RMSn electrogram). Group mean RMS electrogram was constructed from the arithmetic average of the respective RMS electrograms from all dogs. Figure 6 summarizes the effect of acute ischemia on the RMS electrogram calculated from the leads only in the ischemic region. Panel A illustrates the RMSi electrogram of unfiltered epicardial electrograms, in which X axis represents a time from QRS onset determined from the unfiltered electrograms. Panel B shows the RMSi electrogram of the low frequency (0-25Hz) range, in which X axis represents a time from QRS onset determined from the filtered electrograms. Dotted and solid curves represent the group mean RMSi electrograms in all dogs just before coronary occlusion (preRMSi) and 10 minutes after the occlusion (postRMSi), respectively. Dashed curves indicate the difference RMSi electrograms (postRMSi-preRMSi), which were constructed by subtracting the mean RMSi electrograms before coronary occlusion (preRMSi) from those after coronary occlusion (postRMSi). In the difference RMSi electrograms, positive value represents the time point where RMSi values were increased after coronary occlusion, while negative value represents the time point where fAQRST value were decreased after coronary

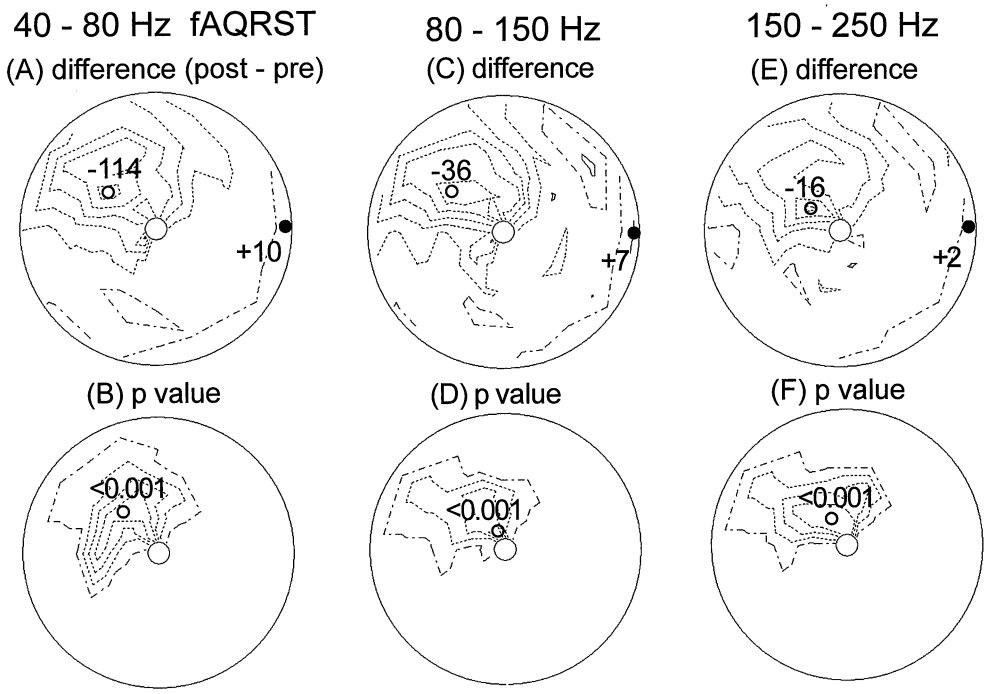

Figure 5 Effect of ischemia on 40-80, 80-150, and 150-250 Hz fAQRST maps.
Only difference map (post-pre), and p value map (pre vs. post) were displayed.

occlusion compared to those before occlusion. Mean values of postRMSi were compared statistically line by line with the mean values of preRMSi by the use of ANOVA with Scheffe's test. Solid boxes under the curve indicate the significant difference between the mean values of postRMSi and preRMSi at that time. Each step represents $p<0.05$, $p<0.01$, and $p<0.001$, respectively.

Figure 6A illustrates the effect of ischemia on signal-averaged nonfiltered RMSi electrogram. After coronary occlusion, QRS widening accompanied by the elevation of ST segment was observed. In addition, the slope of initial QRS complex was less steep, and the peak R wave amplitude was increased in the ischemic phase. Figure 6B illustrates effects of ischemia on low frequency (0-25Hz) RMSi electrogram. The pattern of 0-25Hz RMSi electrogram was similar to unfiltered RMSi electrogram. Low frequency (0-25Hz) components were detectable throughout the QRS complex, ST segment, and T wave. Acute myocardial ischemia produced a significant attenuation of 0-25Hz RMSi voltages in the early portion of QRS complex (in the area from 7 to 20 msec after QRS onset). On the other hand, RMSi voltages calculated from the last half of the QRS complex and early ST segment (in the range from 35 to 102 msec after QRS onset) were increased significantly after occlusion.

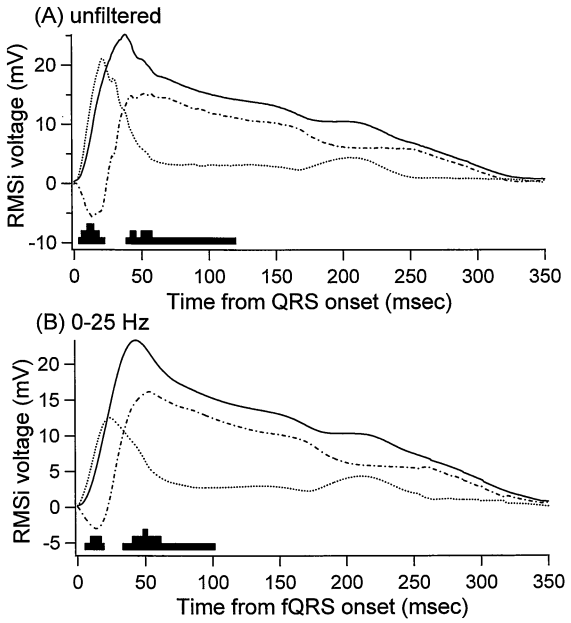

Figure 6 Effect of ischemia on RMSi electrograms calculated from the leads only in the ischemic region.

Panel A illustrates the RMSi electrogram calculated from signal-averaged nonfiltered epicardial electrograms, and panel B shows the RMSi electrogram of low frequency (0-25Hz) range. Dotted and solid curves represent the mean RMSi electrograms of just before coronary occlusion (preRMSi) and 10 minutes after occlusion (postRMSi), respectively. Dashed curves indicate the difference of the mean RMSi electrograms (postRMSi - preRMSi). Solid boxes under the curve indicate the significant difference between postRMSi and preRMSi at that time. Each step represents $p<0.05$, $p<0.01$, and $p<0.001$, respectively.

RMSi : root-mean-square voltage calculated from the leads in the ischemic region.

fQRS : filtered QRS complex

Figure 7 represents effects of acute ischemia on mid- and high-frequency RMSi electrograms. Group mean RMSi electrograms were constructed from an arithmetic average of the respective fAQRST values from all dogs. To investigate the changes of RMSi values especially in the terminal QRS, the reference point for averaging was set to the offset of the filtered QRS complex before coronary occlusion. Individual RMSi electrograms from all dogs were aligned at this reference point, and averaged together. Because the QRS duration was slightly different among animals, it was difficult to assess the changes of voltages in the terminal QRS, if individual RMSi electrograms from different dogs were aligned at the point of each QRS onset.

Figure 7A and B represents the change in mid-frequency (25-40, and 40-80Hz) RMSi electrograms, respectively. These frequency components contributed to the terminal QRS and were also detectable throughout the QRS complex and early ST segment. Myocardial ischemia significantly attenuated the mid-frequency RMSi voltages in the initial to middle segment of the QRS complex. After LAD occlusion, mid-frequency RMSi values were increased slightly at the terminal QRS, however these changes were not statistically significant.

Figures 7C and D represent high-frequency (80-150, and 150-250Hz) RMSi electrograms, respectively. These high frequency potentials were detected throughout the QRS complex. Myocardial ischemia significantly diminished the high-frequency (80-150, and 150-250Hz) RMSi voltages in the area from an

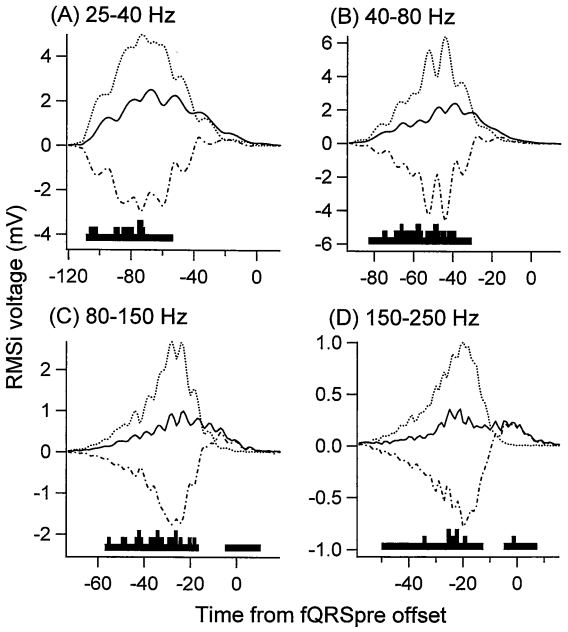

Figure 7 Effect of ischemia on the RMSi electrograms of mid-and high-frequency ranges calculated from the leads only in the ischemic region.
fQRSpre : filtered QRS complex in the control phase.

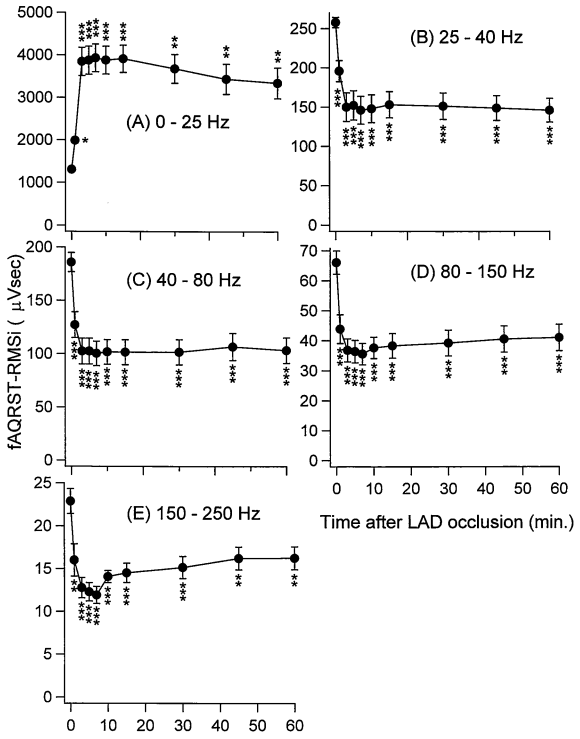

Figure 8 Time course of fAQRST-RMSi values.
From a beginning to end of entire cardiac cycle, time integration of RMSi electrogram was calculated and referred to as fAQRST-RMSi. The figure shows time course of fAQRST-RMSi values based on leads in the ischemic region recorded just before and after occlusion. Time scales are the same for all graphs. Direct lines were drawn between each two adjacent points.
* ; $p<0.05$, ** ; $p<0.01$, *** ; $p<0.001$ vs. control by ANOVA and Dunnett test.
LAD : left anterior descending coronary artery,
fAQRST-RMSi: filtered QRST area of RMSi electrogram.

early to middle portion of the QRS complex. Alternatively, myocardial ischemia significantly increased the high frequency (80-150, and 150-250 Hz) RMSi voltages in the terminal portion of the QRS complex (Figs. 7C, D). However, no significant changes were found in RMSn electrograms of all 5 frequency ranges in the non-ischemic region (data not shown in the figures).

Time course of changes in each frequency component

Throughout the entire cardiac cycle, time integration of RMS electrogram was calculated and referred to as fAQRST-RMS in this paper. Values of fAQRST-RMS represent an overall amplitude of each frequency component in the entire cardiac cycle. Sixty-lead epicardial electrograms were recorded every 3 minutes for 10 times prior to coronary occlusion. There were no significant changes in fAQRST-RMS values in the control phase (data not shown in the figure).

Figure 8 illustrates the time course of fAQRST-RMS values based on leads only in ischemic region (fAQRST-RMSi) recorded just before and after LAD occlusion. Mean values of fAQRST-RMSi after occlusion were compared statistically with the mean values of just before occlusion by the use of ANOVA and post hoc testing with the Dunnett connection. As can be seen, low frequency (0-25Hz) fAQRST-RMSi value was significantly increased after LAD occlusion (panel A). One minute after occlusion, 0-25Hz fAQRST-RMSi value was increased moderately, and it almost reached maximum plateau level about 3 minutes after the occlusion. Mean values of 0-25Hz fAQRST-RMSi after occlusion showed a gradual buildup to 300.7% of the control value.

Both mid- and high-frequency (25-40, 40-80, 80-150, and 150-250Hz) fAQRST-RMSi values were significantly decreased after LAD occlusion (panel B, C, D, and E). One minute after occlusion, each fAQRST-RMSi value was decreased moderately, and it almost reached minimum plateau level about 3 minutes after the coronary occlusion. Mean values of

mid- and high-frequency (25-40, 40-80, 80-150, and 150-250Hz) fAQRST-RMSi showed marked decreases and reached 56.7, 53.6, 53.9, and 52.1% of each control value, respectively. In contrast, in the non-ischemic region, no significant changes were observed in fAQRST-RMS values of all 5 frequency ranges (data not shown in figures).

Discussion

Spatial distributions of each frequency component

Mor-Avi and coworkers[1] recorded epicardial electrogram from the ischemic region in dogs, and performed the time-domain analysis on the epicardial electrogram. They reported that peak-to-peak amplitude of the high-frequency (150 to 250Hz) epicardial signals within the QRS complex was decreased significantly after LAD occlusion. They also performed frequency domain anlysis[4] of the entire QRS complex in epicardial electrograms, and revealed that the power in the mid- and high-frequency range (40-150, 150-250Hz) was decreased, while the power in the low-frequency range (2-40Hz) was increased after coronary occlusion. However, in these studies, epicardial electrograms were recorded with two bipolar electrodes placed in the ischemic left ventricular region and in the non-ischemic right ventricle, and the epicardial spatial distribution of each frequency component is not investigated so far. In addition, there have been few studies about the effect of myocardial ischemia on the temporal distributions of both high- and low-frequency potentials of epicardial electrogram.

First, we examined the effect of acute myocardial ischemia upon the epicardial distribution of each frequency component. In this study, it was demonstrated that in the ischemic region, overall low-frequency potentials of the entire cardiac cycle (0-25Hz fAQRST) were significantly increased after coronary occlusion (Fig. 3), and acute myocardial ischemia markedly reduced both mid- and high-frequency potentials (25-40, 40-80, 80-150, and 150-250Hz fAQRST) (Figs. 4 and 5). However, in the non-ischemic region, there were no significant changes in all the 5 frequency components. Basically, the results of this study are in general agreement with those reported by the previous studies[1-4]. They reported that the power in the range of 2-40Hz was increased after coronary occlusion[4]. In contrast, we revealed that in the ischemic region, the overall low frequency (0-25Hz) potentials of entire cardiac cycle were increased after the occlusion, while overall potentials in the frequency range of 25-40Hz were decreased after occlusion.

On the other hand, Nichols et al.[10] reported that after coronary ligation, location of the peak high frequency QRS component was shifted to a site overlying the ischemic damage, and a secondary site of increased high frequency QRS component emerged on the opposite surface, possibly reflecting a reciprocal effect. The results of their study were different from that reported in our present study. In our study, the high frequency QRS component was reduced in the infarct zone, and a reciprocal effect was not observed in the non-infarct zone. However the reason why the results of our study were different from that reported in their studies is unclear, we speculate that differences in methodology may cause the contrary results. They performed harmonic analysis of QRS complex and constructed an isoharmonic map, and reported that high frequency QRS components were increased relatively in the ischemic zone. However, in their study, it is unclear that the high frequency QRS components were increased absolutely or the proportion of the components was increased relatively due to the reduction of the low frequency components. In contrast, we demonstrated that the high frequency QRS potentials were decreased absolutely in the infarct zone. Further studies should be needed to examine the effect of acute myocardial ischemia on each frequency component of the QRS complex.

Temporal distributions of each frequency component

There have been few studies about changes in temporal distributions of epicardial high-frequency QRS potential by acute myocardial ischemia. Mor-Avi et al.[1] reported that in the body surface lead, high frequency (150-250Hz) potentials were reduced in the

mid portion of QRS complex during LAD occlusion. However, in their study, changes in temporal distributions of epicardial high-frequency QRS potentials are unclear. So, we investigated the effect of acute ischemia on the temporal distributions of the low-, mid- and high-frequency epicardial QRS potentials.

In the present study, acute myocardial ischemia caused a marked attenuation of low-frequency (0-25Hz) RMSi voltages only in the early portion of QRS complex (Fig. 6B). In addition, the slope of initial QRS complex in the unfiltered electrogram became less steep in the ischemic phase compared with that in the control phase (Fig. 6A). It was suggested that myocardial ischemia caused a reduced conduction velocity due to a reduced slope of a fast depolarization phase of the action potential, and then diminished the low-frequency component in the initial QRS.

On the other hand, low frequency (0-25Hz) RMSi voltages calculated from the last half of the QRS complex and ST segment were increased significantly after LAD occlusion (Fig. 6B). This finding may suggest that myocardial ischemia caused the widening of the QRS complex, the increase in an amplitude of the peak R wave, and the elevation of the ST segments (Fig. 6A), and then increased the low-frequency components in the last half of the QRS complex and ST segment. It was also revealed that the overall low-frequency potentials of entire cardiac cycle (0-25Hz fAQRST-RMSi) were increased after the occlusion, because the increase in the 0-25Hz RMSi values in the last half of the QRS complex and ST segment was larger than the decrease in those in the initial QRS (Figs. 6 and 8).

In contrast, acute myocardial ischemia significantly attenuated both the mid- and high-frequency potentials (25-40, 40-80, 80-150, 150-250Hz RMSi voltages) in the area from the early to middle portion of the QRS complex (Fig. 7). We speculate that a reduction in a depolarization rate of the myocardial cells and a decrease in the conduction velocity as a result of ischemia caused the reduction of mid- and high-frequency potentials in the early to middle portion of the QRS complex. Alternatively, myocardial ischemia significantly increased the high-frequency potentials (80-150, 150-250Hz RMSi voltages) in the terminal portion of the QRS complex. This finding may reflect the slowed, fractionated activation wavefronts induced by myocardial ischemia. It was also demonstrated that the overall high-frequency potentials of entire cardiac cycles (80-150, 150-250Hz fAQRST-RMSi) were decreased after occlusion, because the decrease in the high frequency component in the early and middle portion of the QRS complex was larger than the increase in those in the terminal QRS.

Clinical implications

Clinical importance of high-frequency components within QRS complex lies in its power to detect myocardial ischemia. There are several clinical studies about the high-frequency mid-QRS potentials in the body surface ECG. High-frequency mid-QRS potential was increased after successful percutaneous transluminal coronary angioplasty (PTCA)[2, 21, 22]. In addition, an increase in the amplitude of the high-frequency components of the QRS complex occurred with successful reperfusion following thrombolytic therapy in acute myocardial infarction[23, 24]. High-frequency signal-averaged ECG may be helpful in the noninvasive diagnosis of the effectiveness of these therapies. The methods and results of the present study will be useful clinically to improve the diagnostic power to evaluate myocardial ischemia with body surface signal-averaged ECGs. In the previous studies[2, 21-24], overall amplitude of the high frequency (150-250Hz) potentials throughout the QRS complex was examined in the bipolar X, Y, and Z orthogonal ECGs. In the present study, it was suggested that the reduction of mid- and high-frequency potentials in the early to middle QRS complex may reflect the extent of myocardial ischemia. The measurement of mid- and high-frequency potentials solely in the early to middle QRS in the ischemic leads by signal-averaged standard 12-lead ECG or body surface ECG mapping system may improve the diagnostic accuracy to detect the myocardial ischemia. It was also speculated that

the increase in high-frequency potentials in the terminal QRS may reflect the risk of malignant ventricular arrhythmia during acute ischemia. Future experimental and clinical studies must be needed to prove the above-mentioned hypothesis. In addition, to investigate the effects of acute myocardial ischemia on the body surface distributions and temporal distributions of each frequency QRS potential, further clinical studies should be needed.

Conclusions

Acute myocardial ischemia significantly reduced the low-frequency (0-25Hz) potentials only in the initial QRS, whereas markedly increased these components especially in the last half of QRS complex and ST segment. In contrast, myocardial ischemia significantly decreased the mid- and high-frequency (25-250Hz) potentials in the early to middle portion of the QRS complex, while markedly increased the high-frequency (80-250Hz) components in the terminal QRS complex.

References

1) Mor-Avi V., Shargorodsky B., Abboud S., Laniado S., Akselrod S. : Effects of coronary occlusion on high frequency component of the epicardial electrogram and body surface electrocardiogram. *Circulation* 76, 237-243, 1987.

2) Abboud S., Cohen R.I., Selwyn A., Ganz P., Sadeh D., Friedman P.L. : Detection of transient myocardial ischemia by computer analysis of standard and signal-averaged high-frequency electrocardiograms in patients undergoing percutaneous transluminal coronary angioplasty. *Circulation* 7, 585-596, 1987.

3) Abboud S. : Subtle alterations in the high-frequency QRS potentials during myocardial ischemia in dogs. *Computers & Biomedical Research* 20, 384-395, 1987.

4) Mor-Avi V., Akselrod S. : Spectral analysis of canine epicardial electrogram. Short-term variations in the frequency component induced by myocardial ischemia. *Circulation Research* 66, 1681-1691, 1990.

5) Goldberger A.L., Bhargava V., Froelicher V., Covell J., Mortara D. : Effect of myocardial infarction on the peak amplitude of high frequency QRS potentials. *Journal of Electrocardiology* 13, 367-371, 1980.

6) Goldberger A.L., Bhargava V., Froelicher V., Covell J. : Effect of myocardial infarction on high frequency QRS potentials. *Circulation* 64, 34-42, 1981.

7) Bhargava V., Goldberger A. : Myocardial Infarction diminishes both low and high frequency QRS potentials : Power spectrum analysis of lead II. *Journal of Electrocardiology* 14, 57-60, 1981.

8) Hosoya Y., Kubota I., Shibata T., Yamaki M., Ikeda K., Tomoike H. : Spectral analysis of 87-lead body surface signal-averaged ECGs in patients with previous anterior myocardial infarction as a marker of ventricular tachycardia. *Circulation* 85, 2060-2064, 1992.

9) Hosoya Y., Ikeda K., Komatsu T., Yamaki M., Kubota I. : Spectral analysis of epicardial 60-lead electrograms in dogs with 4-week-old myocardial infarction. *Journal of Electrocardiology* 34, 14-24, 2001.

10) Nichols T.L., Mirvis D.M. : Frequency component of the electrocardiogram. Spatial features and effects of myocardial infarction. *Journal of Electrocardiology* 18, 185-194, 1985.

11) Novak P., Li Z., Novak V., Hatala R. : Time-frequency mapping of the QRS complex in normal subjects and in postmyocardial infarction patients. *Journal of Electrocardiology* 27, 49-60, 1994.

12) Simson M.B. : Use of signals in terminal QRS complex to identify patients with ventricular tachycardia after myocardial infarction. *Circulation* 64, 235-242, 1981.

13) Shibata T., Kubota I., Ikeda K., Tsuiki K., Yasui S. : Body surface mapping of high-frequency components in the terminal portion during QRS complex for the prediction of ventricular tachycardia in patients with previous myocardial infarction. *Circulation* 82, 2084-2092, 1990.

14) Kelen G.J., Henkin R., Starr A.M., Caref E.B., Bloomfield D., el-Sherif N. : Spectral turbulence analysis of the signal-averaged electrocardiogram

and its predictive accuracy for inducible sustained monomorphic ventricular tachycardia. American *Journal of Cardiology* 67, 965-975, 1991.

15) Slavkovsky P., Hulin I. : Gliding-window fast Fourier transform analysis of the entire QRS complex and the distribution of area ratio peaks in healthy subjects and patients with myocardial infarction. *Coronary Artery Disease* 5, 249-256, 1994.

16) Kubota I., Yamaki M., Shibata T., Ikeno E., Hosoya Y., Tomoike H. : Role of ATP-sensitive K+ channel on ECG ST segment elevation during a bout of myocardial ischemia. *Circulation* 88, 1845-1851, 1993.

17) Konta T., Ikeda K., Yamaki Y., Nakamura K., Honma K., Kubota I., Yasui S. : Significance of discordant ST alternans in ventricular fibrillation. *Circulation* 82, 2185-2189, 1990.

18) Hanashima K., Kubota I., Ozawa T., Shibata T., Yamaki M., Ikeda K., Yasui S. : Effect of altered activation sequence on epicardial QRST area and refractory period in dogs. *Circulation* 84, 1346-1353, 1991.

19) Kubota I., Hosoya Y., Shibata T., Yamaki M., Ikeda K., Tomoike H. : Spectral analysis of the first half QRS complex in normal subjects and patients with previous myocardial infarction. *American Journal Noninvasive Cardiology* 6, 104-108, 1992.

20) Abboud S. : High-frequency electrocardiogram analysis of the entire QRS in the diagnosis and assessment of coronary artery disease. *Progress in Cardiovascular Diseases* 35, 311-328, 1993.

21) Berkalp B., Oral D., Caglar N., Omurlu K., Pamir G., Alpman A., Erol C., Kervancioglu C., Akgun G., Akyol T. : Effects of percutaneous transluminal coronary angioplasty on late potentials and high frequency mid-QRS potentials. *Cardiology* 85, 216-221, 1994.

22) Pettersson J., Lander P., Pahlm O., S ○ rnmo L., Warren S.G., Wagner G.S. : Electrocardiographic changes during prolonged coronary artery occlusion in man : comparison of standard and high-frequency recordings. *Clinical Physiology* 18, 179-186, 1998.

23) Aversano T., Rudikoff B., Washington A., Traill S., Coombs V., Raqueno J. : High frequency QRS electrocardiography in the detection of reperfusion following thrombotic therapy. *Clinical Cardiology* 17, 175-182, 1994.

24) Xue Q., Reddy B.R., Aversano T. : Analysis of high-frequency signal-averaged ECG measurements. *Journal of Electrocardiology* 28 Suppl., 239-245, 1995.

Received : October 31, 2001.

Accepted : January 4, 2002.